中国石油大学(华东)
CHINA UNIVERSITY OF PETROLEUM

OMICS Group Conferences
Accelerating Scientific Discovery

International Conference on Geology

地球科学与技术学院
School of Geosciences

油气储层研究中心
Petroleum reservoir research center

诚 实 做 人 踏 实 做 事

International Conference on Geology-2015

Coupling of dynamics and physical property in hydrocarbon accumulation period control the oil-bearing property of low permeability turbidite reservoir

Yang Tian   Cao Yingchang Wang Yanzhong

China university of petroleum. School of Geoscience

June 22 2015 Orlando Florida

Outline

- Introduction
- Geological background
- Materials and methods
- Characteristics and petrophysical evolution of low permeability turibite reservoirs
- Petrophysical constraint of turbidite reservoirs in the accumulation period
- Factors that control relationship strengths between property and dynamics of a reservior in accumulation period
- Conclusions

Introduction

With the increasing interest for oil and gas exploration and development, low permeability clastic rock reservoirs become the key prospecting target areas

The low permeability rock reservoirs have gone through complex diagenetic events, The distribution of sandstone porosity is inconsistent with the hydrocarbon accumulation

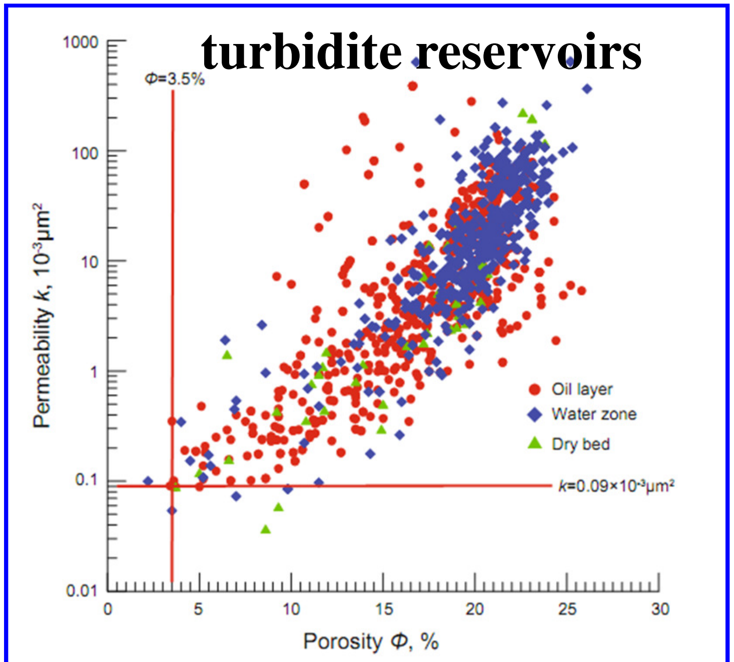

The high or low physical property sandstone reservoirs either contain oil or not

The comparison between permeability and the petrophysical constraints of turbidite reservoirs in the accumulation period is the most important factor for the distribution of the oil bearing property of reservoirs today.

hypothesis

Geological background

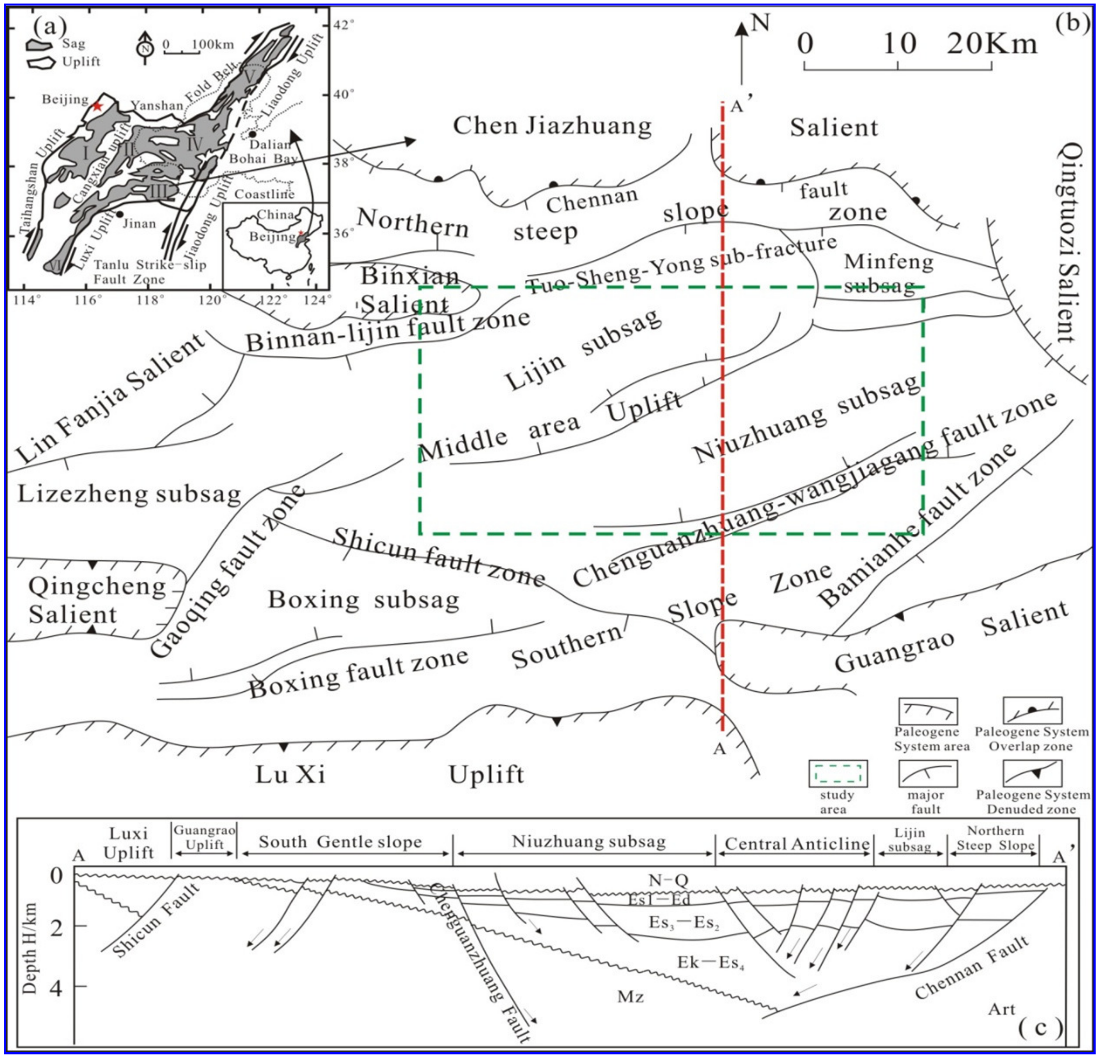

Structural map of Dongying Sag. The area in the green line is the study area (After Liu et al, 2014)

The Dongying Sag is a sub-tectonic unit lying in the southeastern part of the Jiyang Depression of the Bohai Bay Basin, East China.

It is a half graben with a faulted northern margin and a gentle southern margin. In plan, this sag is further subdivided into several secondary structural units, such as the northern steep slope zone, middle upliftbelt, and the Lijin, Minfeng, Niuzhuang trough zones, Boxing subsags, and the southern gentle zone (Zhang et al, 2014).

Geological background

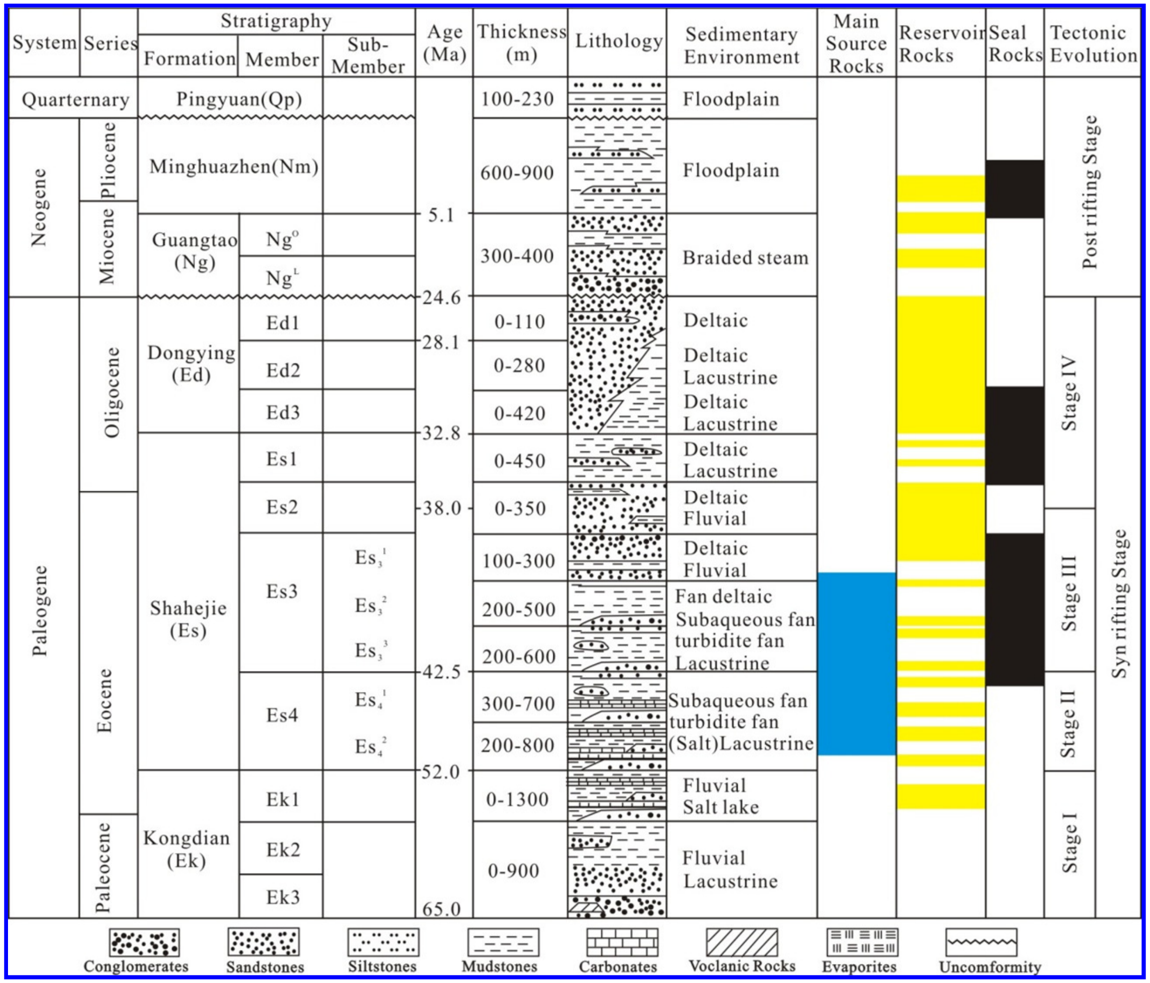

Generalized Cenozoic Quaternary stratigraphy of the Dongying Sag, showing tectonic and sedimentary evolution stages and the major petroleum system elements (After Yuan et al, 2015)

The sag is filled with Cenozoic sediments, which are formations from the Paleogene, Neogene, and Quaternary periods. The formations from the Paleogene period are the Kongdian (Ek), Shahejie (Es), and Dongying (Ed); the formations from the Neogene period are the Guantao (Ng) and Minghuazhen (Nm); and the formation from the Quaternary period is the Pingyuan (Qp).

Geological background

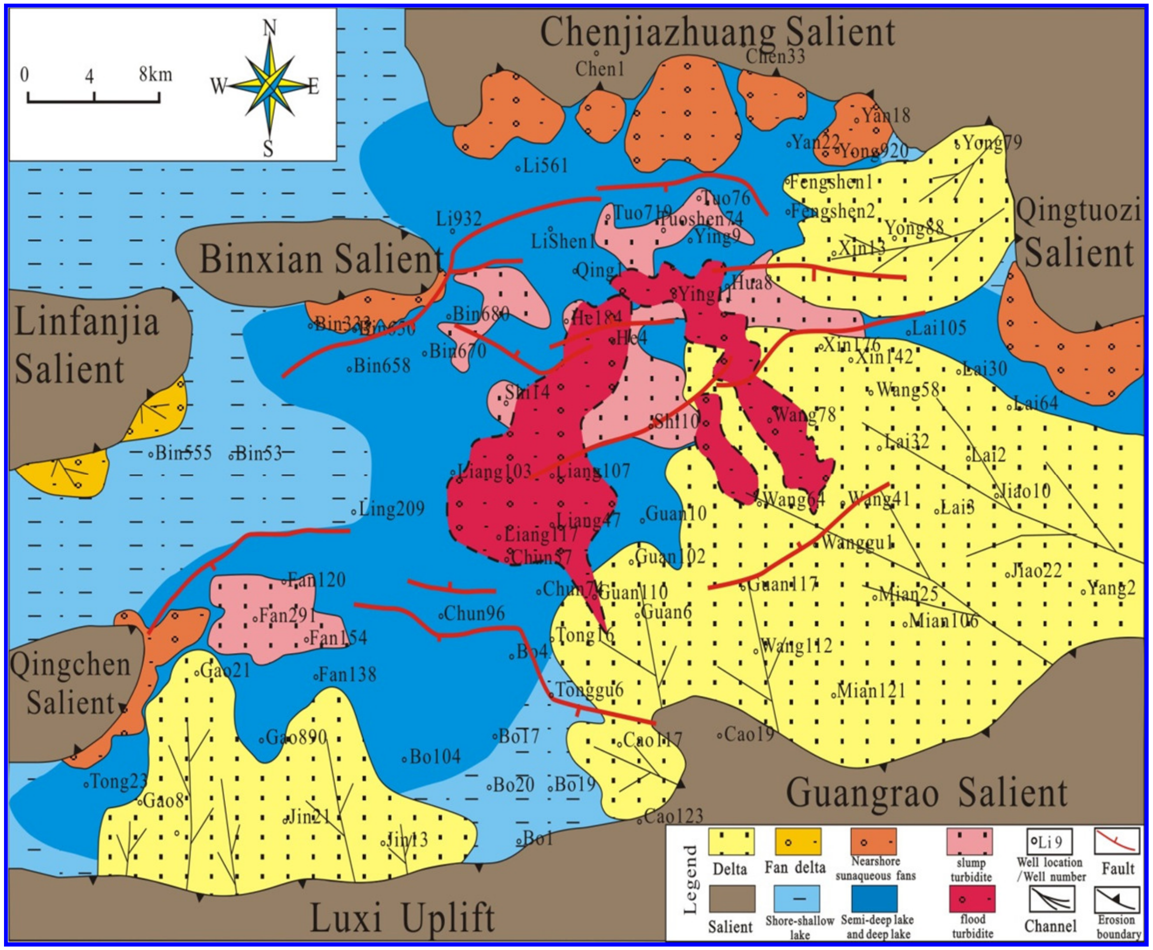

Sedimentary faciess distribution of Es3z in Dongying sag

During the depositon of the third member of Shahejie formation, tectonic movement was strong, and the basin subsided rapidly reaching the maximum depth. Therefore, large amounts of detrital materials were transported into the basin and formed plentiful source rock and turbidite in deep-water environment in hollow zone and uplifted zone. Most turbidite reservoirs are low permeability reservoir with complex oil-bearing characteristics and the studies are controversial.

Materials and methods

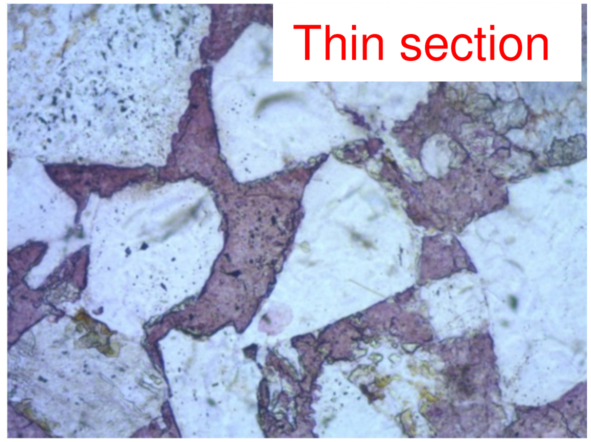

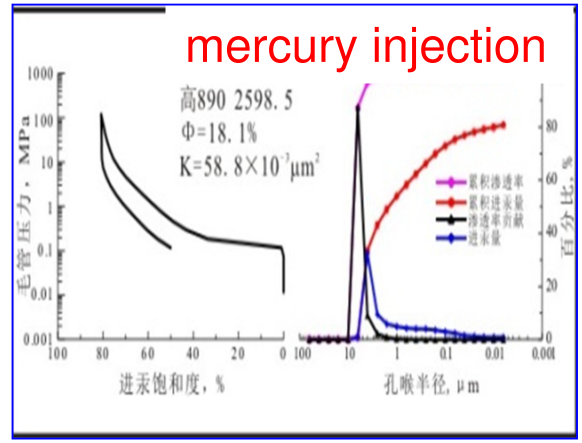

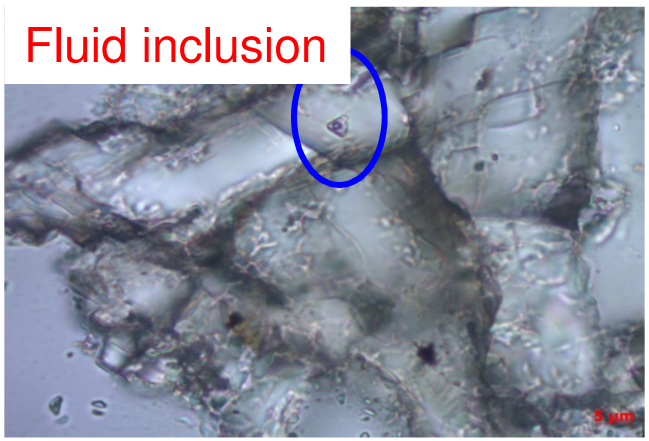

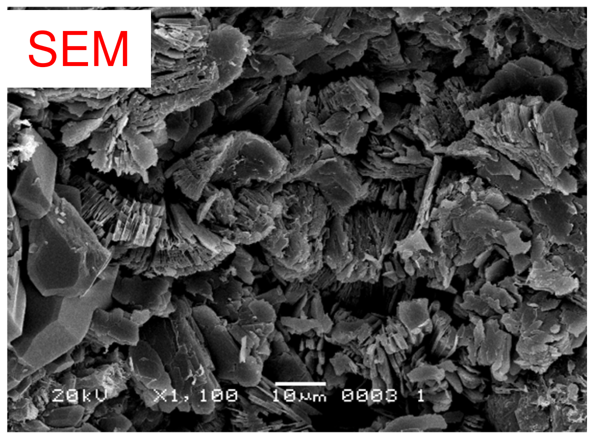

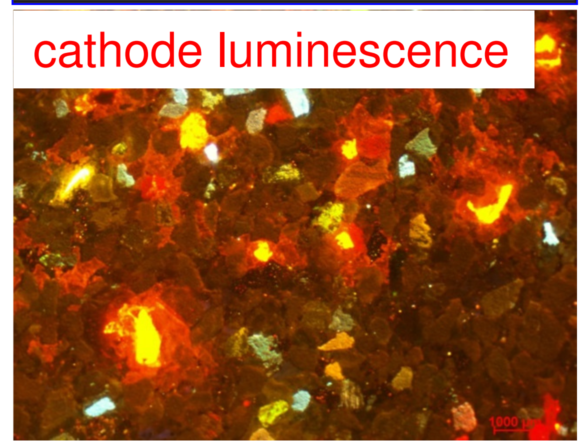

Over 1500 maters representative core of turbidite in the aim formation have been descripted. After 119 typical samples drilling from the core, analysis and test items include thin sections testing with 119 samples, measured property testing with 119 samples, mercury injection testing with 90 samples, scanning electron microscopy (SEM) testing with 15 samples, cathode luminescence testing with 17 samples, fluorescence thin section testing with 17 samples, and fluid inclusion testing with 53 samples have been carried out.

Characteristics and petrophysical evolution

- Petrography

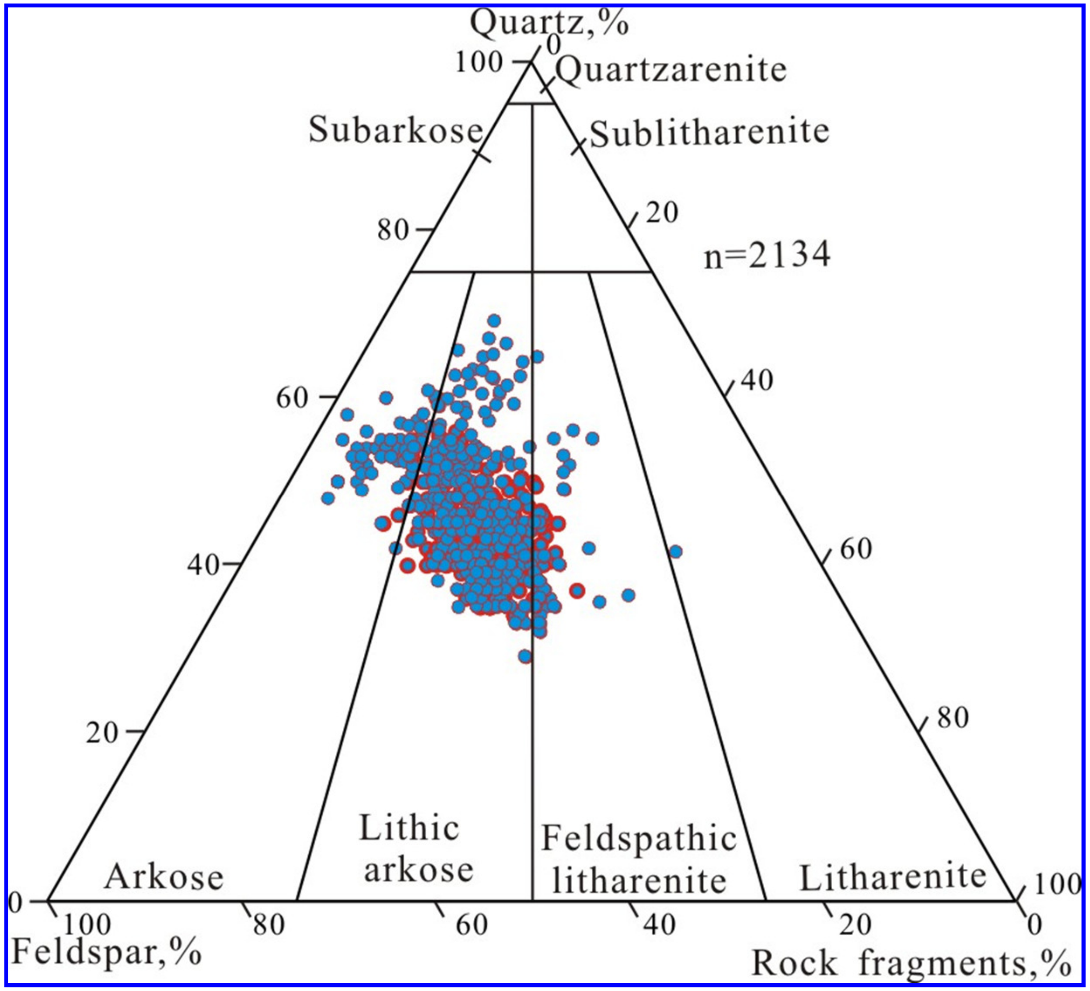

Triangular plot of rock types of the low permeability turbidite reservoir

- fine to medium grained
- quartz 29%-69.2%
- feldspar 14.3%-47%
- the detritus content is 2%-44.2
- mud content is 0.5%-48%
- the cement content is 0.5%-34.6 %
- compositional maturity is 0.414-2.247
- moderately sorted
- with sub-angular or sub-rounded shapes.

Characteristics and petrophysical evolution

- Porosity-permeability

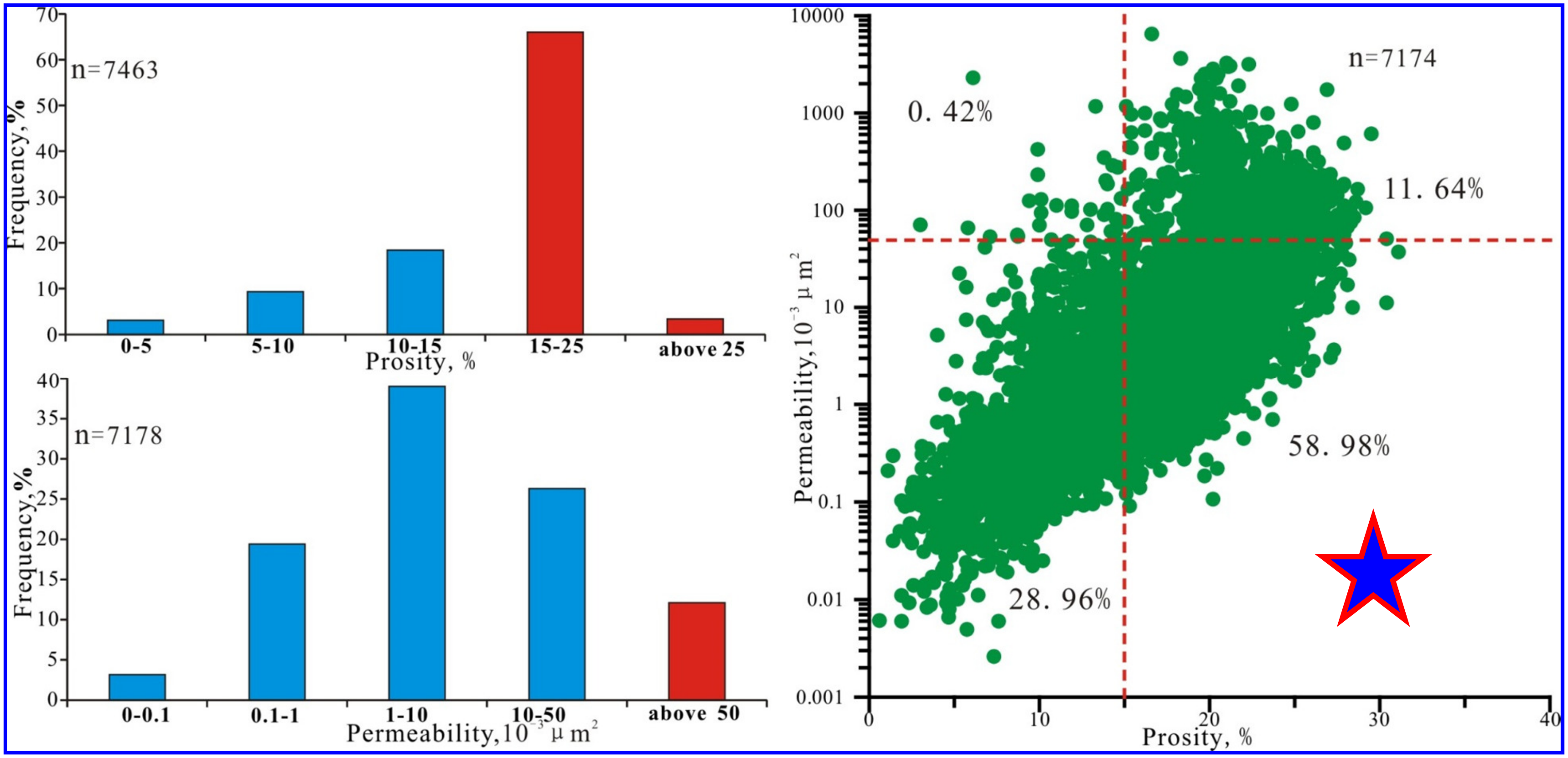

porosity and permeability distribution

With an average porosity value of 17.15%
With an average permeability value of 38.11 × 10^{-3} μm^2
20.82% low porosity reservoirs, 69.18%, middle-high porosity reservoirs,
87.89% low permeability reservoirs and, 12.11% high permeability reservoirs.

Characteristics and petrophysical evolution

➢ Reservoir space

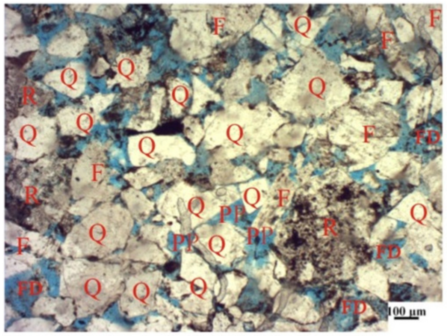

(e) Niu42, 3258.6m (−) ;Grain point contact

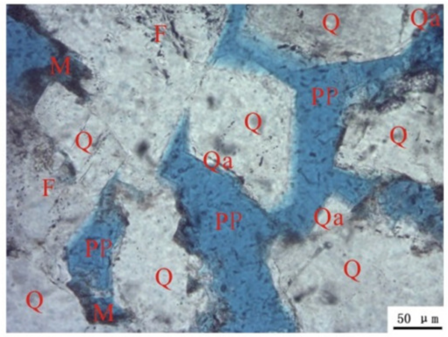

(f) He155, 2987. 04m (−) ; Primarily pore

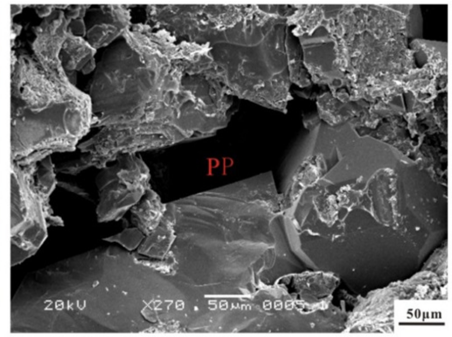

(g) Shi101, 3258. 6m (SE) ; Primarily pore

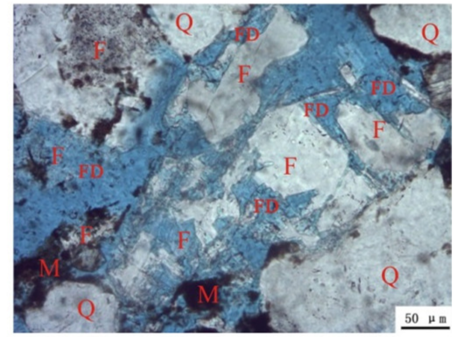

(h) Hao7, 2961. 1m (−) ; Dissolution expand pore

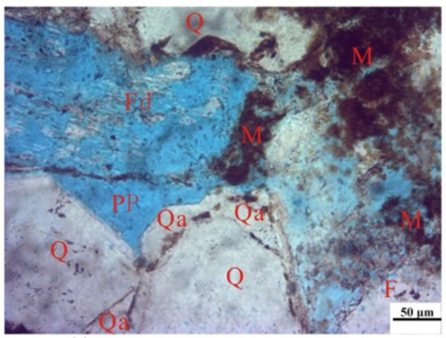

(i) Wangxie 543, 3184. 5m (−) ;
Moldic pore

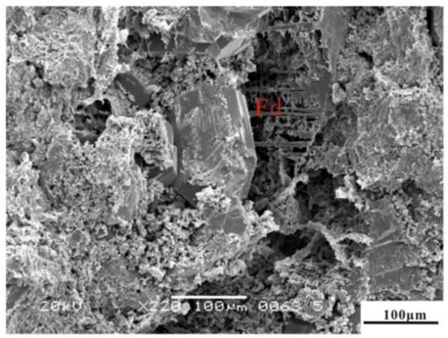

(j) Wangxie 543, 3180. 6m (SE) ;
Feldspar dissolution pore

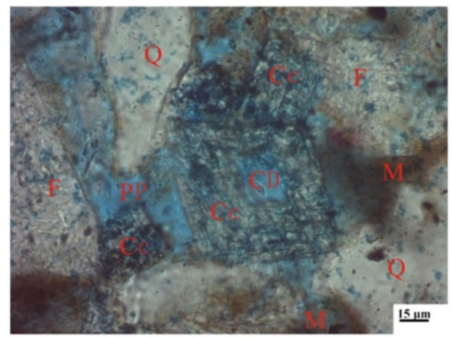

(k) Dongke1, 3333. 65m (−) ;
Ankerite dissolution pore

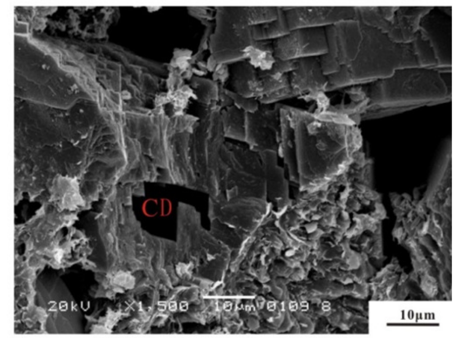

(l) Dongke1, 3333. 65m (SE) ;
Ankerite dissolution pore

Types of reservoir space

- ◆ **The reservoir space contains primary pore, mixed pore , secondary pore and gap.**
- ◆ **Primary pores include the remaining intergranular pore after compaction and cementation and micropores in clay mineral matrix making up the main pore type**
- ◆ **Dissolution expanding pore is the main kind of mixed pore**
- ◆ **There are various kind of secondary pore and gaps containing dissolution pore in particles and cement , moldic pore , intergranular micropores of kaolinite , microfracture and diagenetic contraction fracture.**

Characteristics and petrophysical evolution

- The characteristics of pore throat structure

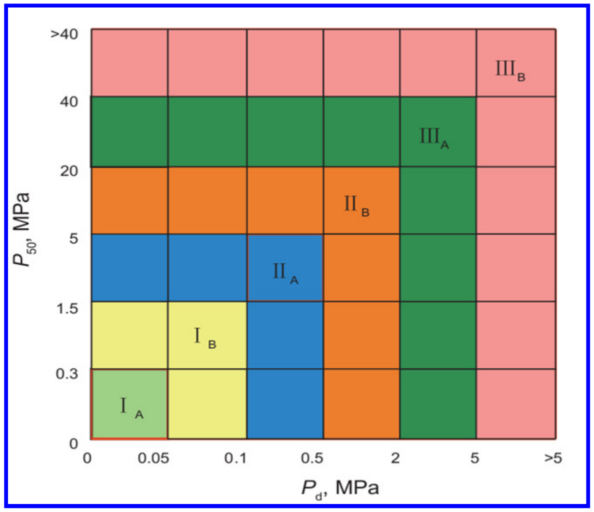

Principle of pore-throat structures classification

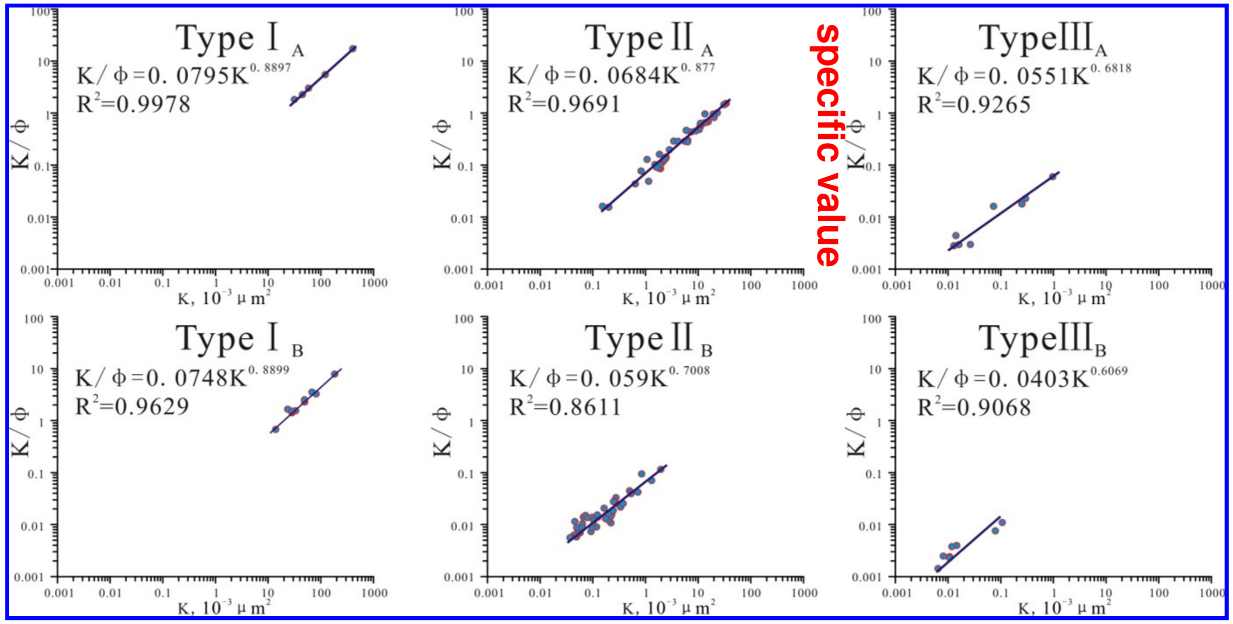

types of pore-throat structures

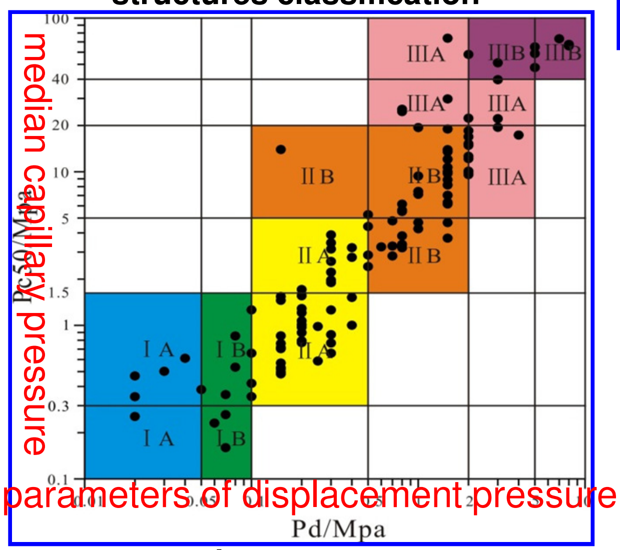

pore-throat structures classification

Type of pore-throat structure	$K/10^{-3}\mu m^2$	K/Φ	P_d/Mpa	P_{50}/Mpa
I A	>30.6	>1.5163	0.02-0.05	0.256-0.611
I B	13.9-183.3371	0.6761-7.8465	0.06-1	0.16-1.263
II A	0.1532-34.3	0.0155-1.5402	0.15-0.5	0.484-4.412
II B	0.037-1.9498	0.00561-0.1155	0.15-2	2.843-22.349
IIIA	0.0129-0.963	0.00273-0.05791	0.8-4	17.363-74.117
IIIB	<0.109	<0.01086	3-8	47.801-73.529

Physical property distribution of different types of pore-throat

Characteristics and petrophysical evolution

➢ Diagenesis features

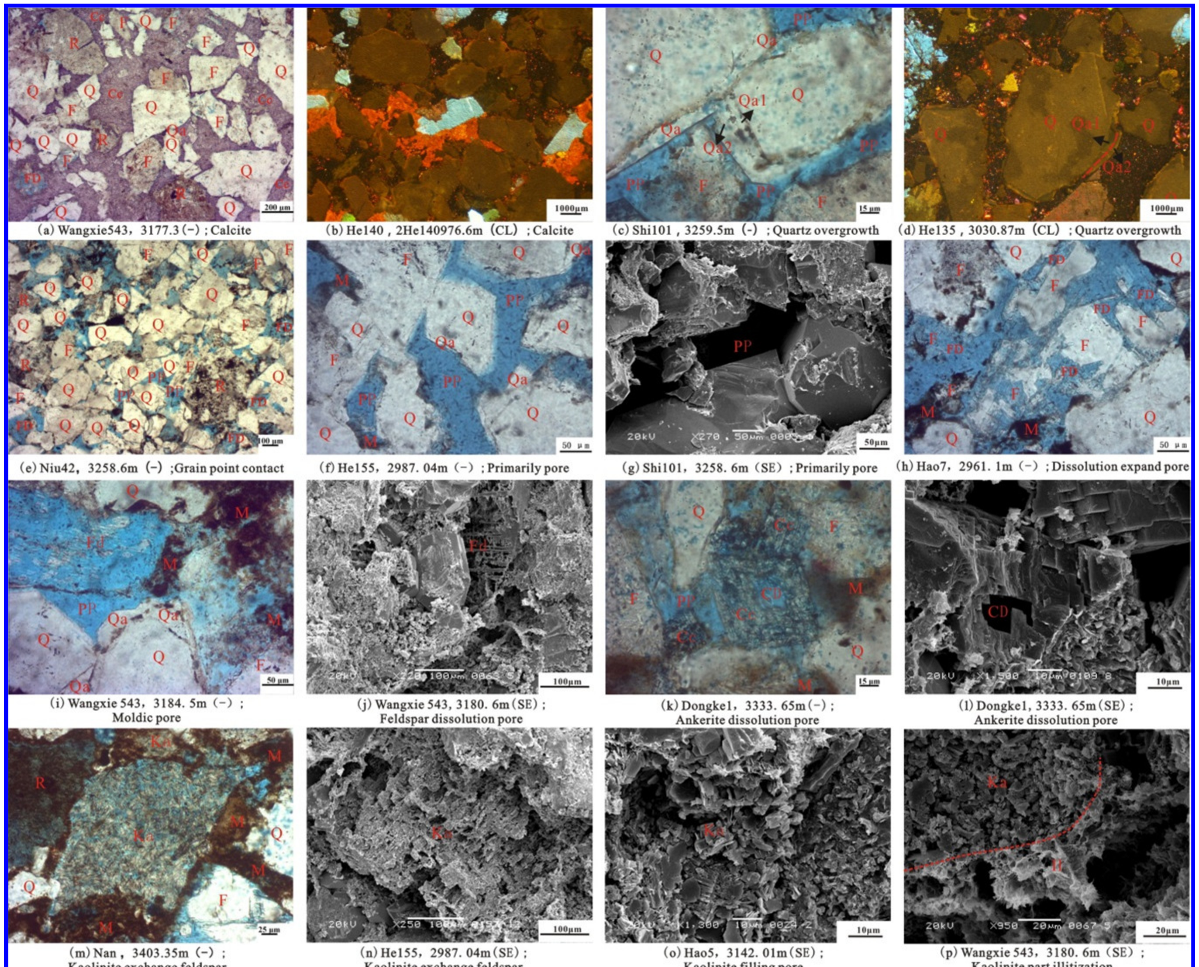

Q-Quartz；F-Feldspar；R-Rock frangmants；M-Matrix；Qa-Quartz overgrowth；Ka-Kaolinite；Il-Illite；Cc-Carbonate cement；FD-Feldspar dissolution；CD-Carbonate dissolution；PP-Primarily pore；(−) plane-polarized light；(CL) athode luminescencec；(SE) scanning electron microscope

diagenesis characteristics

- **The major diagenetic events in the reservoir research area include compaction, cementation, metasomasis and dissolution.**
- **Grain arranged mainly due to point contacts and point-line contacts are reflecting moderate compaction.**
- **The sandstones are mainly carbonate cemented. The first groups of carbonate cements are calcite and ferroan calcite. The second groups of carbonate cements are dolomite, ankerite.**

Characteristics and petrophysical evolution

- Diagenesis features

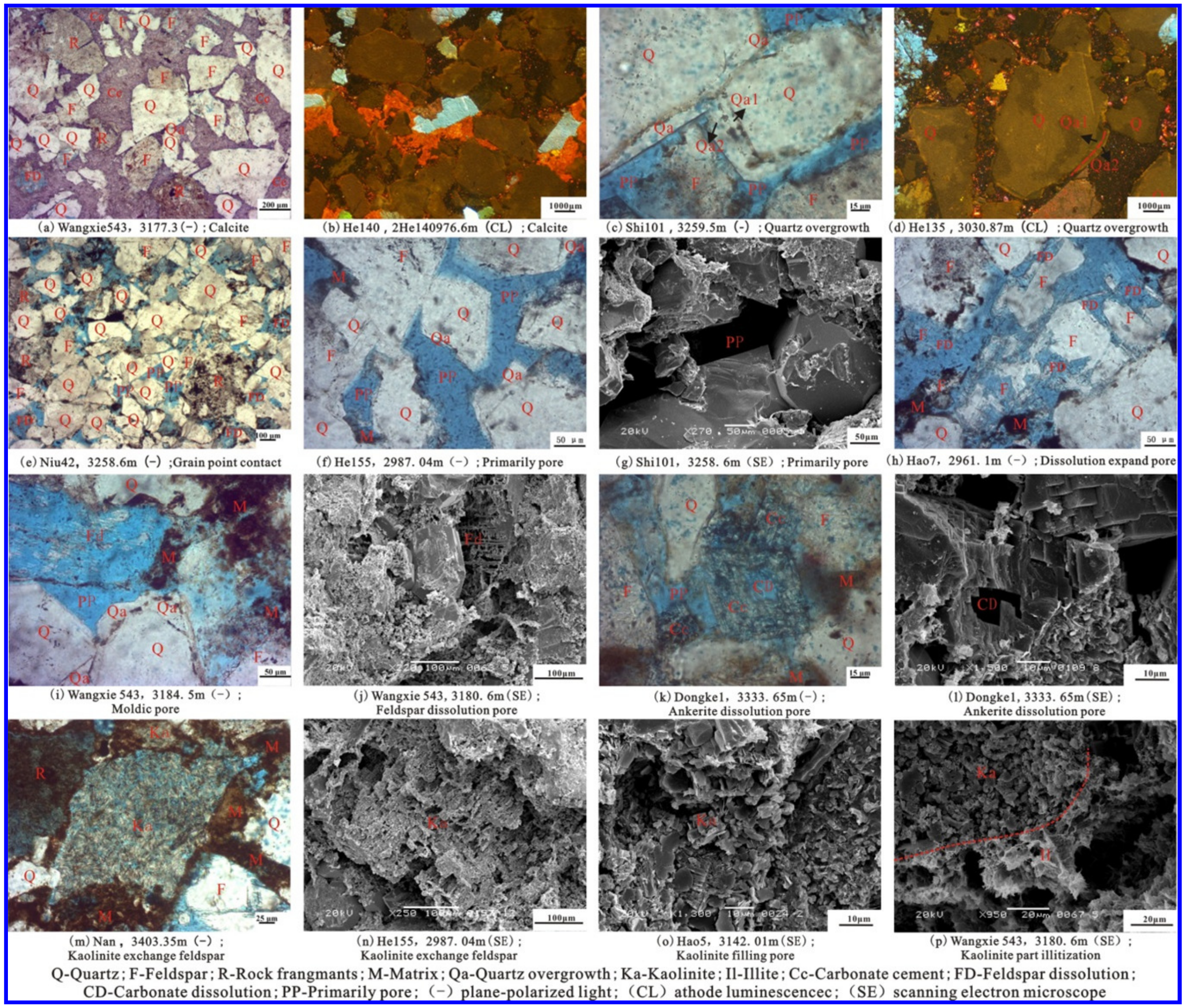

diagenesis characteristics

- **Quartz overgrowth is the main kind of siliceous cementation. Two periods of quartz overgrowth can be identified by cathodoluminescence microscope.**
- **The early period of quartz overgrowth is dark black and the later period is brown .Kaolinite is the most important kind of clay minerals**
- **The dissolution of feldspar, lithic fragment , carbonate cements and other minerals which are unstable in the acid environment can form honeycomb and curved shape dissolution expanding pore**

Characteristics and petrophysical evolution

➢ Paragenesis of Diagenetic minerals

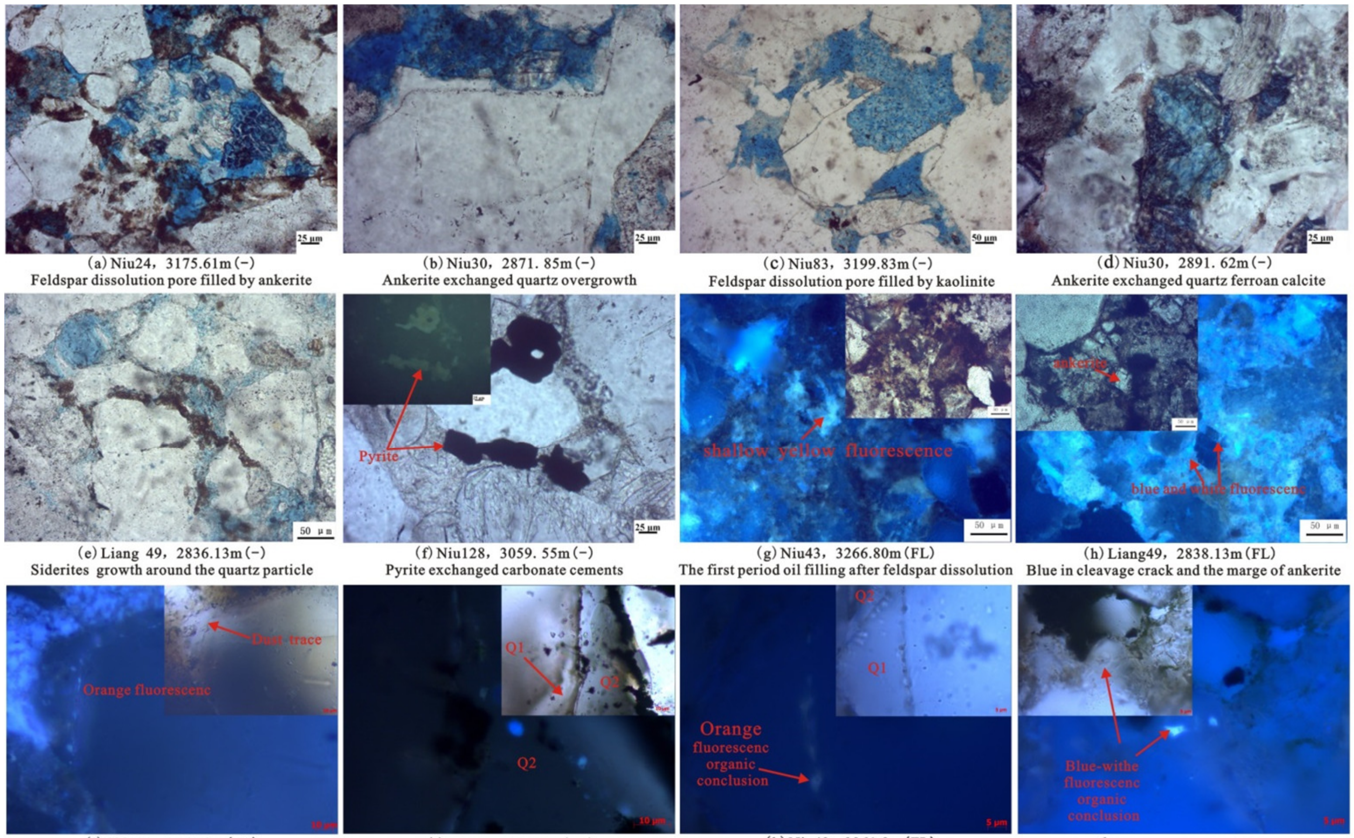

(a) Niu24, 3175.61m (−) Feldspar dissolution pore filled by ankerite
(b) Niu30, 2871. 85m (−) Ankerite exchanged quartz overgrowth
(c) Niu83, 3199.83m (−) Feldspar dissolution pore filled by kaolinite
(d) Niu30, 2891. 62m (−) Ankerite exchanged quartz ferroan calcite
(e) Liang 49, 2836.13m (−) Siderites growth around the quartz particle
(f) Niu128, 3059. 55m (−) Pyrite exchanged carbonate cements
(g) Niu43, 3266.80m (FL) The first period oil filling after feldspar dissolution
(h) Liang49, 2838.13m (FL) Blue in cleavage crack and the marge of ankerite
(i) Shi101, 3263.9m (FL) Orange fluorescenc in quartz overgrowth dust trace
(j) Niu42, 3261.9m (FL) Blue-withe fluorescenc organic conclusion in Q2
(k) Niu42, 3261.9m (FL) Orange fluorescenc organic conclusion in Q1
(l) Nan1, 3401.75m (FL) Blue-withe fluorescenc organic conclusion in ankerite

(−) plane-polarized light; (FL) fluorescence; (Q1) Quarzt overgrowth in the first period; (Q2) Quarzt overgrowth in the second period

On the basis of previous studies (Jiang et al, 2003), two periods of hydrocarbon accumulation can be identified. The first period of hydrocarbon accumulate from 27.5-24.6Ma, and the second period from 13.8-now.

◆ **Metasomasis between carbonate cements ,carbonate cements and clastic ,kaolinite and feldspar ,all occurred. Metasomasis between carbonate cements contains dolomite replaced calcite, ferroan calcite replaced calcite, ankerite replaced calcite and ankerite replaced ferroan calcite.**

Characteristics and petrophysical evolution

- Paragenesis of Diagenetic minerals

early

- Siderite/micritic carbonate
- first dissolution of feldspar
- the beginning of first hydrocarbon filling
- first quartz overgrowth/authigenic kaolinite precipitation
- the second period of carbonate cementation
- the end of first hydrocarbon filling
- dissolution of quartz/feldspar overgrowth
- second dissolution of feldspar and carbonate cementation
- the beginning of second hydrocarbon filling
- second quartz overgrowth/authigenic kaolinite precipitation
- the third period of carbonate cementation/pyrite cementation

later

Compaction existed throughout the whole burial and evolutional processes.

Paragenesis of Diagenetic minerals of turbidite reservoir

Characteristics and petrophysical evolution

➢ petrophysical evolution of low-permeability turbidity reservoirs

permeability recovery method has been employed during the period of geological history of the reservoir

- **Firstly, take the thin sections of the reservoir as study object. After the analysis of the paragenetic sequence and diagenetic fluid evolution, combine with the study of burial history to determine the geological time and burial depth of diagenetic events.**

- **Secondly, fit the function of plane porosity and visual reservoir porosity from the analysis of thin sections, and then we can calculate the contribution in terms of porosity enhancement or decrease of different dissolution pores and authigenic minerals**

- **After the calculation of initial porosity, the evolution of porosity can be recovered with the principle of inversion and back-stripping constraint by Paragenesis of Diagenetic .**

- **Thirdly, the evolution history of actual porosity for geological time can be established quantitatively combined with the mechanical and thermal compaction correction**

- **Fourthly, on the characteristics of pore throat structure, according to back-stripping constraint result of plane porosity and the principle of equivalent expanding the pore throat structures of reservoirs can be recovered.**

- **Finally, according to the relationship between pore throat structure and porosity, the evolution of permeability in geological time can be recovered with the relationship of porosity and permeability in various throat structure.**

Characteristics and petrophysical evolution

- petrophysical evolution of low-permeability turbidity reservoirs

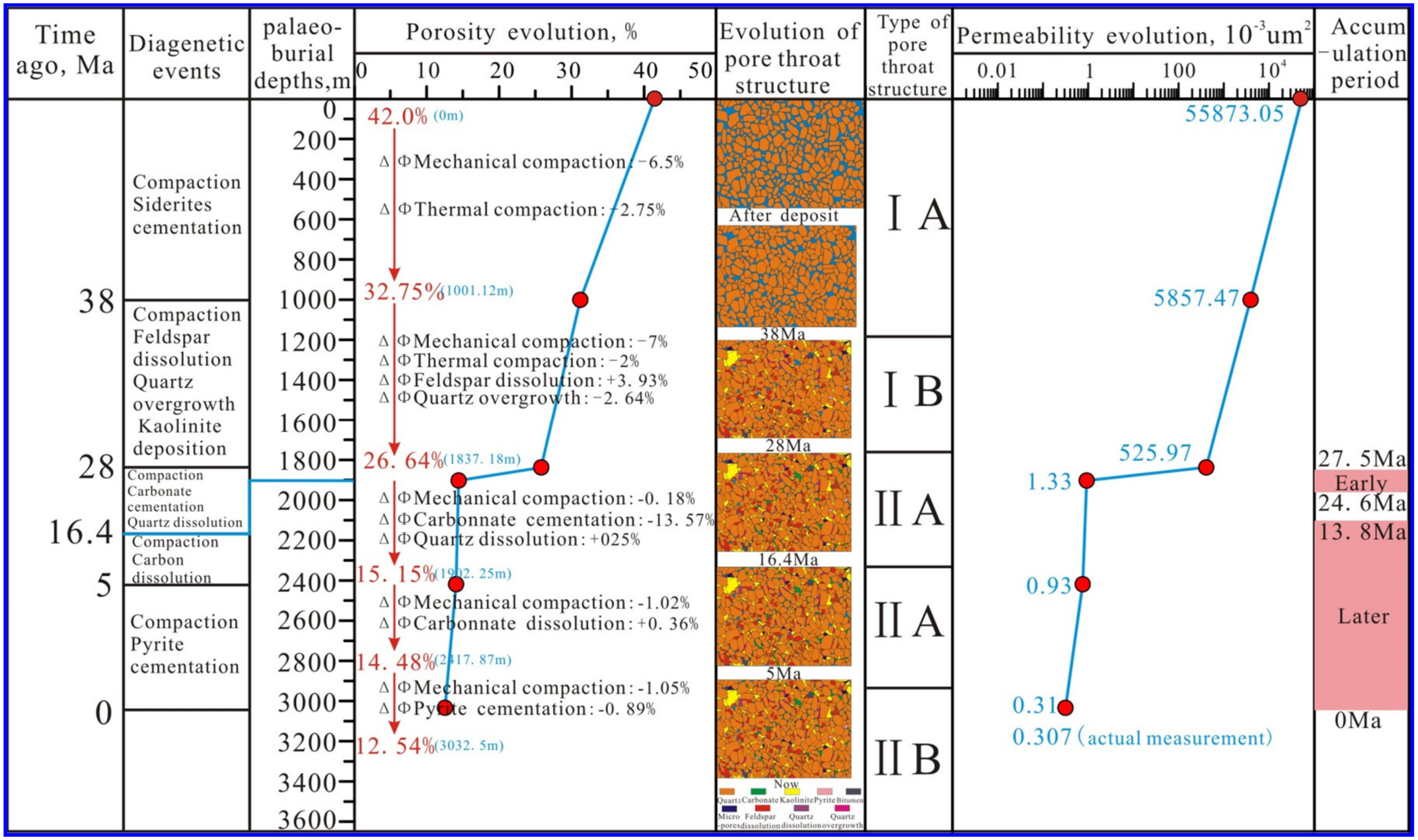

- **Taking the turbidite reservoir of well Niu 107 in 3025.5m as example ,the recovery permeability is 0.31×10⁻³μm² close to the actual measurement permeability 0.307×10⁻³μm². So, this kind of method is accurate and reliable.**

Characteristics and petrophysical evolution

- petrophysical evolution of low-permeability turbidity reservoirs

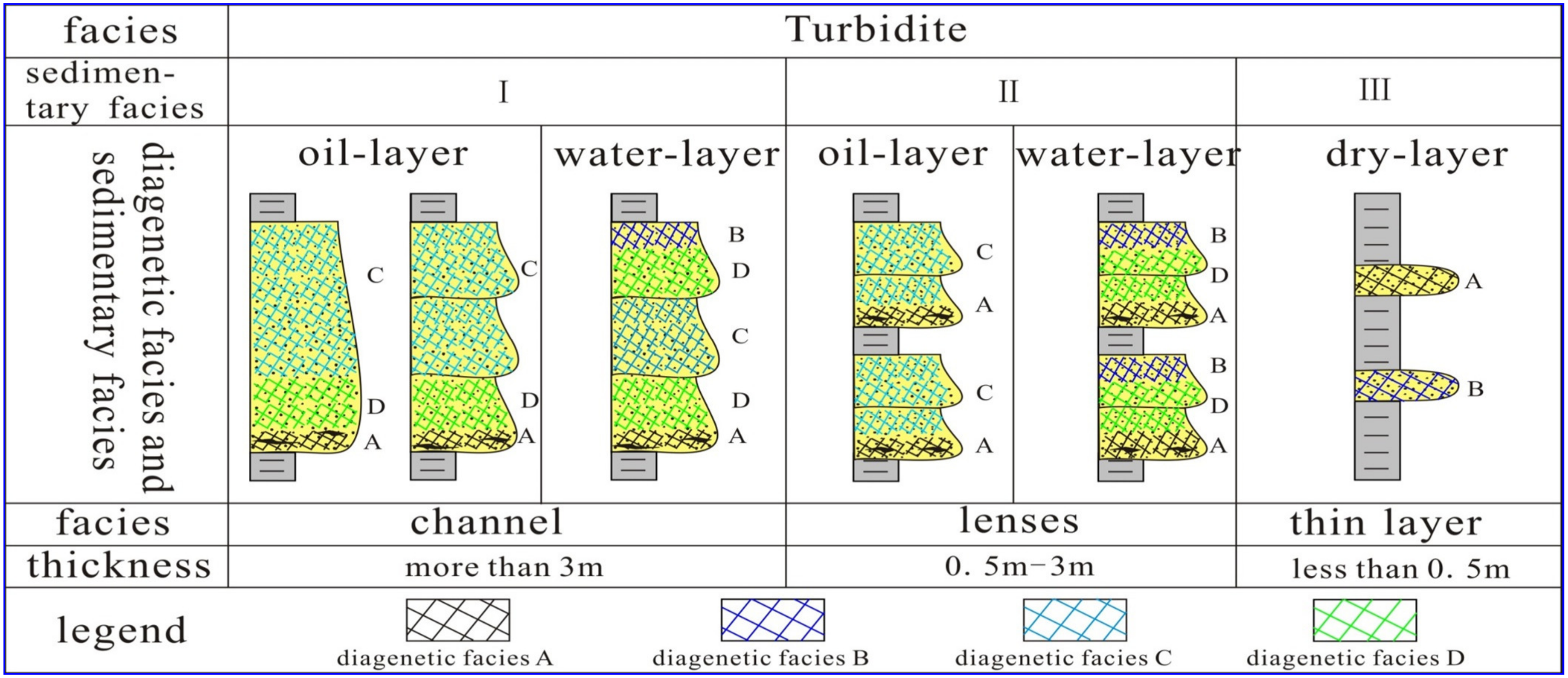

Distribution model of diagenetic facies

- **Thin sandstones mainly develop strong compaction diagenetic facies (A) and strong cementation diagenetic facies (B). Thick sandstones develop diagenetic facies (A) and diagenetic facies (B) in the reservoirs adjacent to mudstones and strong dissolution diagenetic facies (C) and middle dissolution diagenetic facies (D) in the middle of sandstones.**

Characteristics and petrophysical evolution

- petrophysical evolution of low-permeability turbidity reservoirs

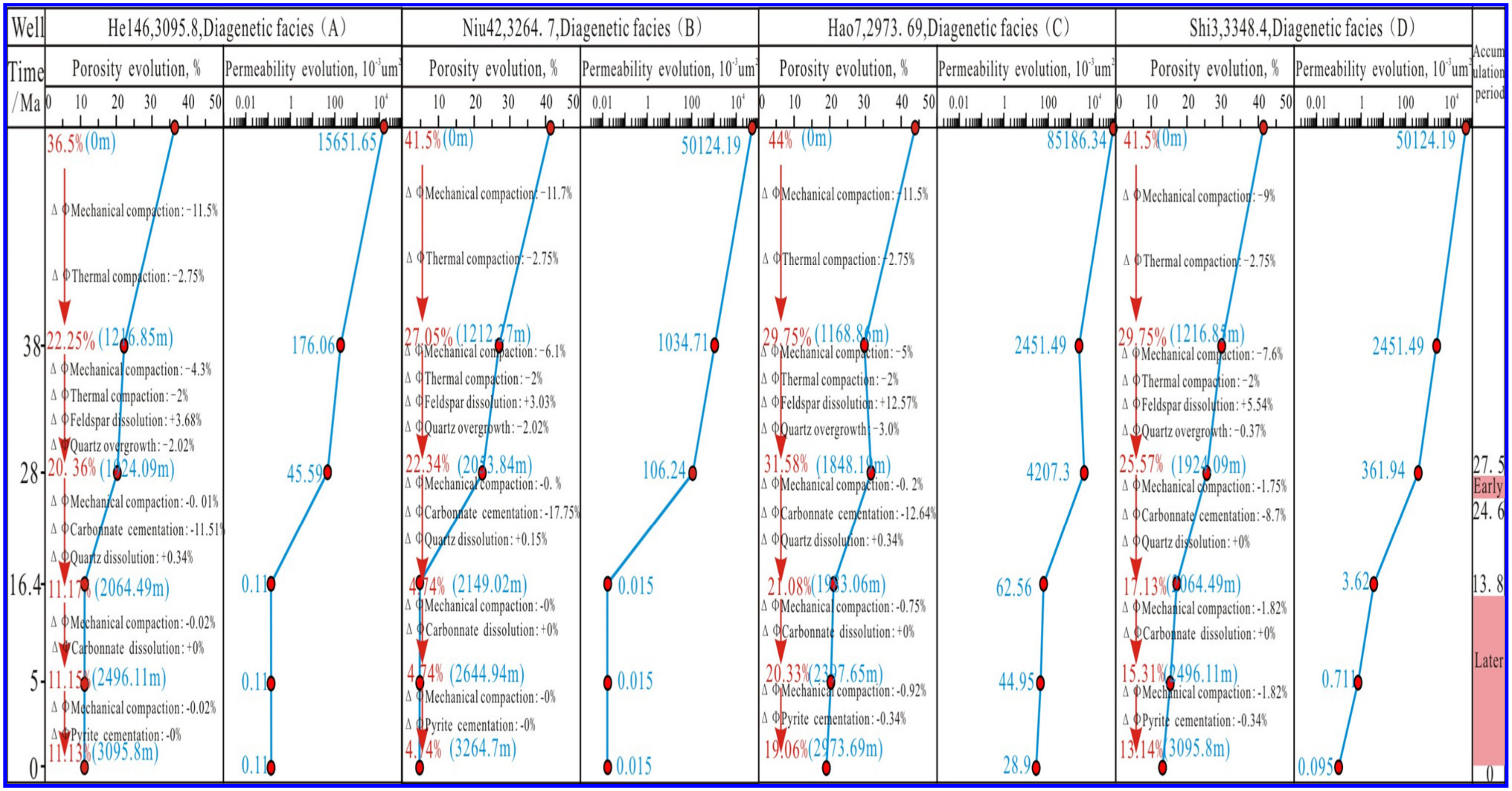

petrophysical evolution of different diagenetic facies

Petrophysical constraint

- Petrophysical constraint of turbidite reservoirs in the accumulation period

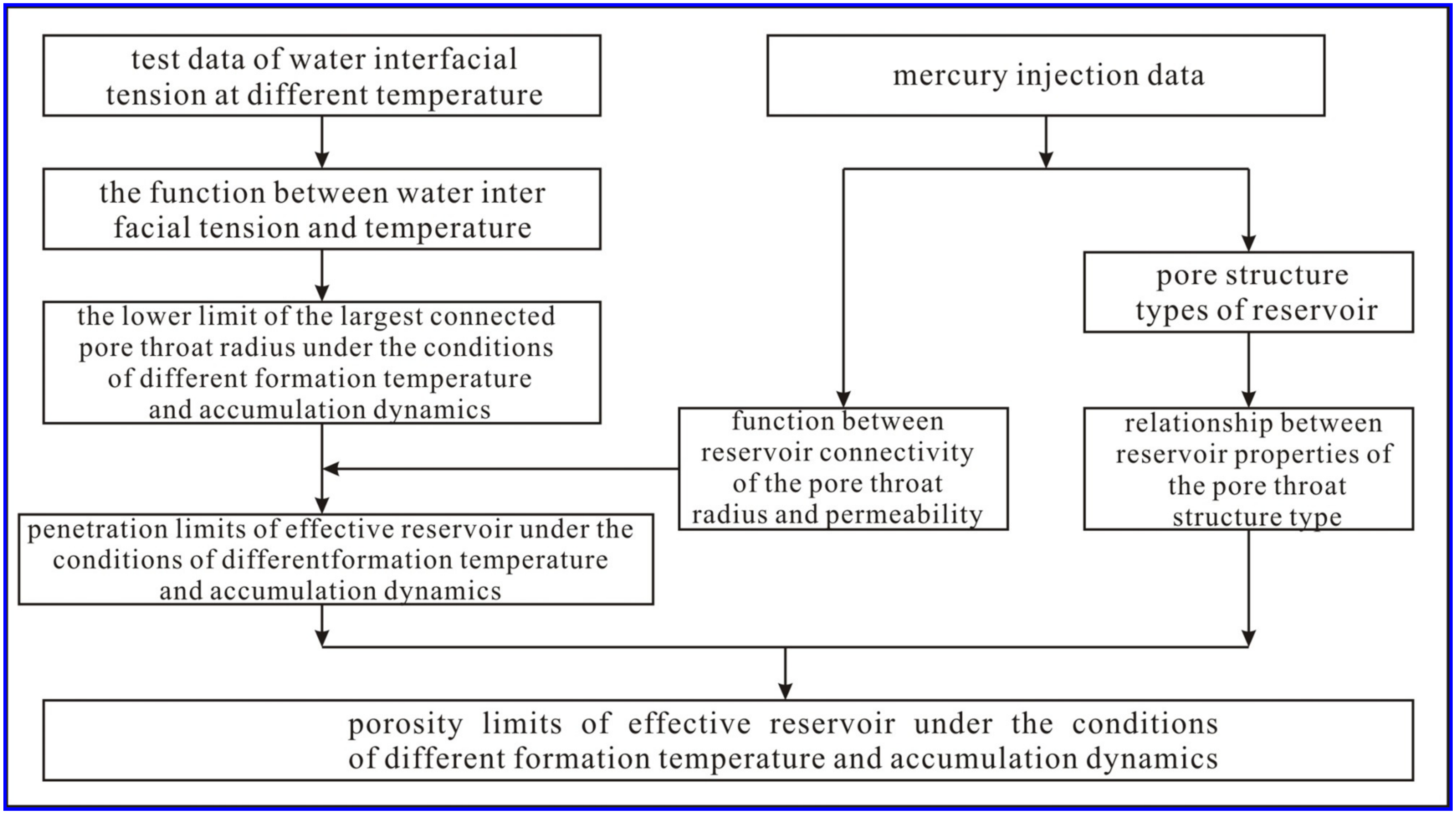

Technology flowchart of the properties of the lower limit under accumulation dynamics and constraints of pore structure in effective reservoir

Petrophysical constraint

- Petrophysical constraint of turbidite reservoirs in the accumulation period

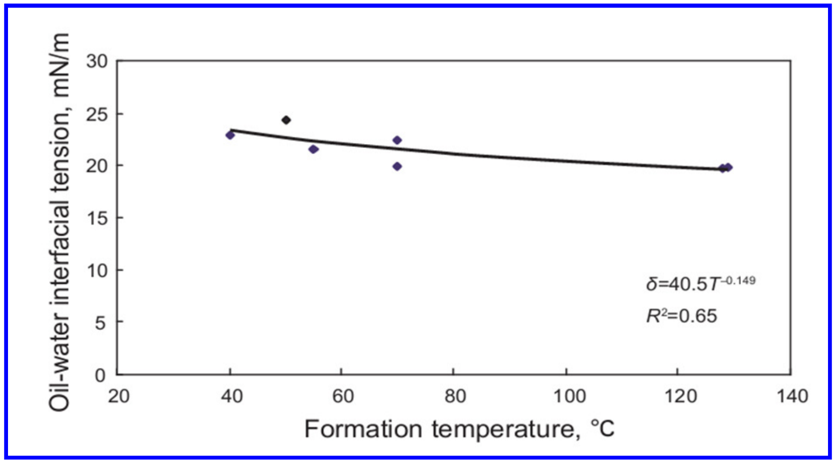

Relationship between oil-water interfacial tension (δ) and formation temperature (T)

$r_0=2\delta\cos\theta/P_f$

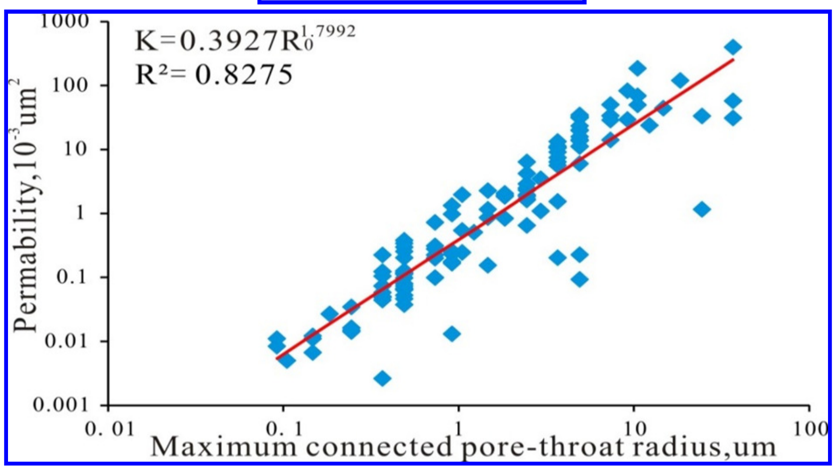

Relationship between permeability and maximum connected pore-throat radius

accumulation dynamics Pf/MPa	Maximum connected pore-throat radius r0/ μ m	Kcutoff /$10^{-3}\mu m^2$	Φcutoff/%					
			Φ Ⅰ A	Φ Ⅰ B	Φ Ⅱ A	Φ Ⅱ B	Φ ⅢA	Φ ⅢB
0.01	48.445	422.819	24.037	——	——	——	——	——
0.02	24.222	121.490	21.616	22.678	——	——	——	——
0.024	20.185	87.514	21.021	21.874	——	——	——	——
0.026	18.633	75.776	20.765	21.530	——	——	——	——
0.03	16.148	58.576	20.315	20.928	——	——	——	——
0.04	12.111	34.908	19.440	19.769	22.632	——	——	——
0.05	9.689	23.365	——	18.914	21.542	——	——	——
0.055	8.808	19.683	——	18.560	21.092	——	——	——
0.06	8.074	16.831	——	18.243	20.690	——	——	——
0.065	7.453	14.573	——	17.956	20.326	——	——	——
0.07	6.921	12.754	——	——	19.996	——	——	——
0.075	6.459	11.265	——	——	19.693	——	——	——
0.08	6.056	10.030	——	——	19.414	——	——	——
0.09	5.383	8.115	——	——	18.914	——	——	——
0.1	4.844	6.714	——	——	18.478	——	——	——
0.2	2.422	1.929	——	——	15.850	20.631	——	——
0.3	1.615	0.930	——	——	14.490	16.585	17.735	——
0.32	1.514	0.828	——	——	14.285	16.019	17.092	——
0.4	1.211	0.554	——	——	13.596	14.206	15.042	——
0.49	0.989	0.385	——	——	12.999	12.736	13.392	——
0.5	0.969	0.371	——	——	12.941	12.598	13.238	——
0.7	0.692	0.203	——	——	12.013	10.511	10.918	——
0.9	0.538	0.129	——	——	——	9.181	9.455	——
1	0.484	0.107	——	——	——	8.675	8.902	10.292
1.2	0.404	0.077	——	——	——	7.864	8.020	9.047
1.4	0.346	0.058	——	——	——	7.237	7.342	8.112
1.5	0.323	0.051	——	——	——	6.974	7.058	7.726
1.6	0.303	0.046	——	——	——	6.736	6.802	7.381
2	0.242	0.031	——	——	——	——	5.986	6.304
2.2	0.220	0.026	——	——	——	——	5.668	5.893
2.4	0.202	0.022	——	——	——	——	5.393	5.541
2.5	0.194	0.021	——	——	——	——	5.268	5.383
3	0.161	0.015	——	——	——	——	4.746	4.732
3.2	0.151	0.013	——	——	——	——	4.574	4.521
3.4	0.142	0.012	——	——	——	——	——	4.331
3.6	0.135	0.011	——	——	——	——	——	4.160
4	0.121	0.009	——	——	——	——	——	3.861
6	0.081	0.004	——	——	——	——	——	2.898
8	0.061	0.003	——	——	——	——	——	2.365
10	0.048	0.002	——	——	——	——	——	2.019

Physical property constraints under the restrain of the accumulation dynamics and pore throat structure of a 125℃ formation temperature

functional relationships between K and K/Φ of different pore-throat structures

Petrophysical constraint

- Petrophysical constraint of turbidite reservoirs in the accumulation period

temperature (T) → *oil-water interfacial tension (δ)* → $r_0=2\delta\cos\theta/P_f$

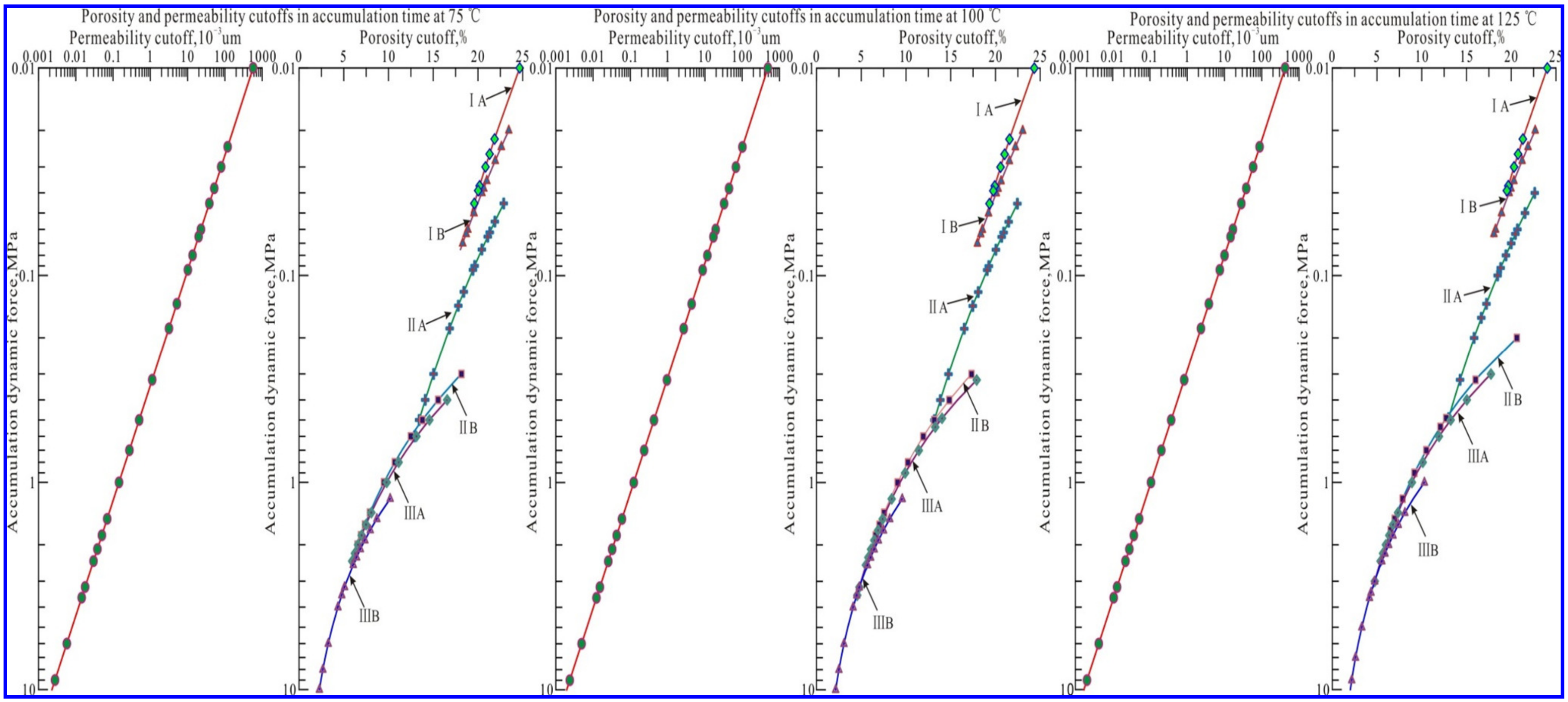

Physical property constraints under different formation temperatures of the low permeability turbidite reservoirs

property and dynamics of a reservior in accumulation period

- Accumulation dynamics recovery

By means of fluid inclusion PVT simulation, the minimum fluid pressure in hydrocarbon accumulation period can be obtained.

Basin modelling technique, fluid pressure after disequilibrium compaction can be determined (the balance pressure between sandstones and mudrocks).

the fluid pressure generated by hydrocarbon generation is 1.4 Mpa to 11.3 Mpa with an average of 5.14 Mpa and the surplus pressure is 1.8 Mpa to 12.6 Mpa with an average of 6.3 Mpa in the early accumulation period

Well	Depth/m	Paleo-fluid pressure /Mpa	Paleopressure after uncompacting /Mpa	Geological time/Ma	palaeoburial depths /m	hydrostatic pressure /Mpa	pressure generate by hydrocarbon /Mpa	surplus pressure /Mpa	The pressure coefficient	accumulation period
Xin154	2936	31.9	31.2	2.3	2800	28	0.7	3.9	1.14	later
Xin 154	2939	22	19.5	27.5	1950	19.5	2.5	2.5	1.13	early
Xin 154	2939	26.8	23.5	7.5	2350	23.5	3.1	3.3	1.14	later
Xin 154	2942.8	29.6	28	2.3	2800	28	--	1.6	1.06	later
Niu 108	3146.5	23.8	22	25.3	2200	22	1.4	1.8	1.08	early
Niu 108	3146.5	33.2	20	11	2000	20	11.6	13.2	1.66	later
Niu 108	3146.5	18.6	20	11	2000	20	--	--	0.93	later
Niu 35	2991.7	22.3	21	9.8	2100	21	0.9	1.3	1.06	later
Niu 107	3272.5	34.6	22.9	9.5	2290	22.9	10.7	11.7	1.51	later
Shi128	3099	33.3	28.5	2.6	2850	28.5	1.1	4.8	1.17	later
Shi 128	3099	27.8	21.4	9.3	2140	21.4	5.8	6.4	1.30	later
Niu 20	3073	43	26.8	3	2680	26.8	12.7	16.2	1.60	later
Niu 20	3073	28.3	21.5	9.1	2150	21.5	5.8	6.8	1.32	later
Niu 24	3159.2	27.9	21.5	25.9	2150	21.5	3.6	6.4	1.30	early
Niu 24	3159.2	29.1	24.5	6	2450	24.5	3.7	4.6	1.19	later
Niu 24	3159.2	32.9	27.1	3.6	2710	27.1	1.7	5.8	1.21	later
Niu 24	3175.6	38.6	26.3	4.7	2630	26.3	11.3	12.3	1.47	later
Niu 24	3175.6	32.2	24	24.8	2400	24	6.9	8.2	1.34	early
Niu 24	3175.6	36.6	24	24.8	2400	24	11.3	12.6	1.53	early
Niu 24	3175.6	27	23.5	9.8	2350	23.5	3.3	3.5	1.15	later
Niu 24	3175.6	26.4	23.5	9.8	2350	23.5	2.7	2.9	1.12	later

Accumulation dynamics recovery of the low permeability turbidite reservoirs

The fluid pressure generated by hydrocarbon generation is 0.7 Mpa to 12.7 Mpa with an average of 5.36 Mpa and the surplus pressure is 1.3 Mpa to 16.2 Mpa with an average of 6.55 Mpa in the later accumulation period.

property and dynamics of a reservior in accumulation period

- The dynamics and physical property coupled with regard to hydrocarbon accumulation period

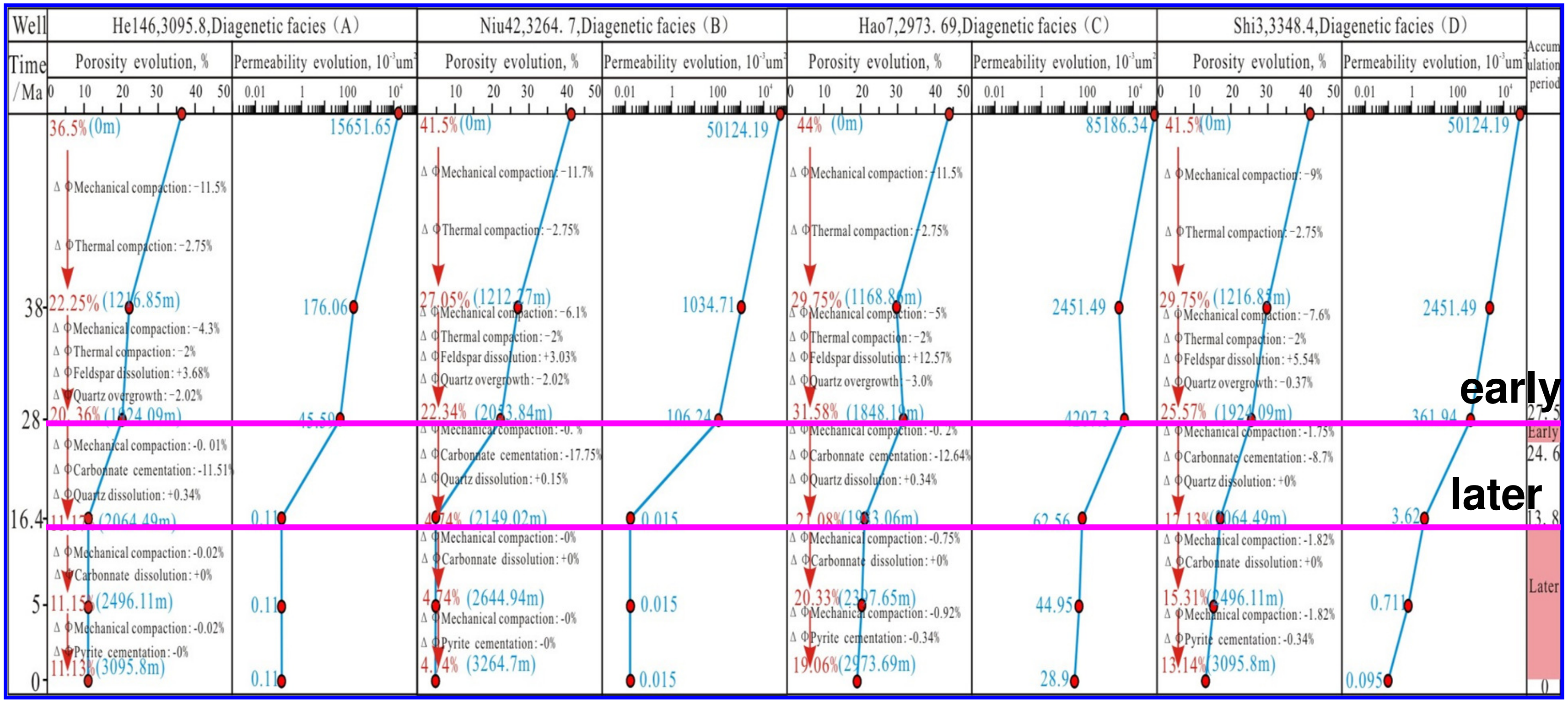

Property evolution of low-permeability turbidity reservoirs in geological time

$10 \times 10^{-3}\mu m^2$ to $4207.3 \times 10^{-3}\mu m^2$ in the early accumulation period

$0.015 \times 10^{-3}\mu m^2$ to $62 \times 10^{-3}\mu m^2$ in the later accumulation period

property and dynamics of a reservior in accumulation period

- The dynamics and physical property coupled with regard to hydrocarbon accumulation period

Petrophysical constraint

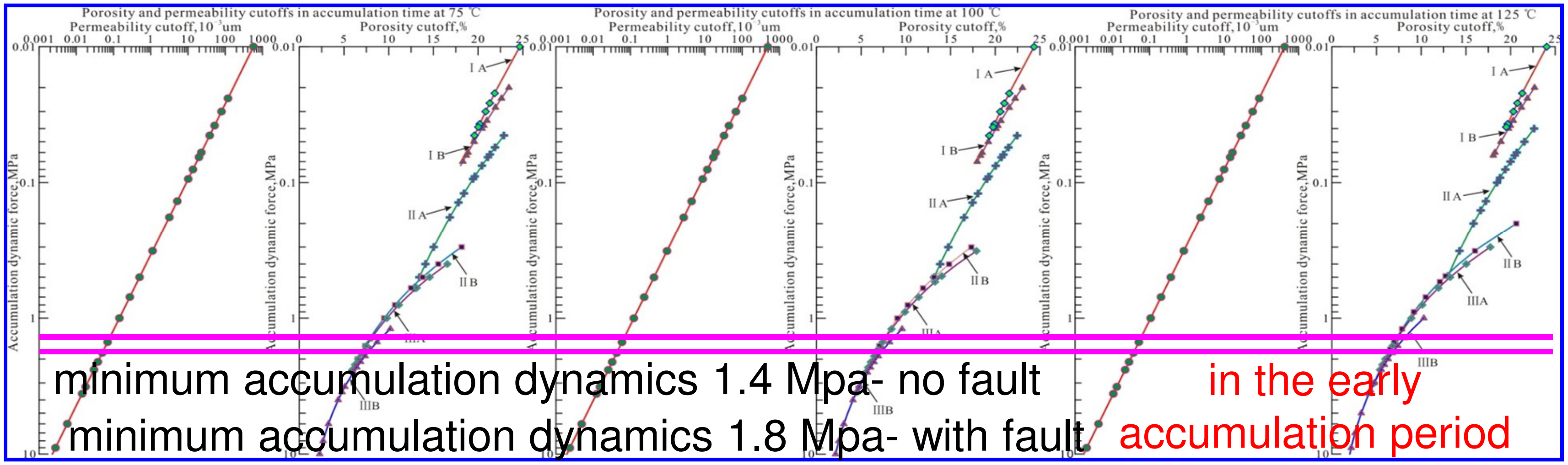

$10\times10^{-3}\mu m^2$ to $4207.3\times10^{-3}\mu m^2$ in the early accumulation period

no fault- the pressure generated by hydrocarbon generation is the main accumulation dynamics. It is 1.4 Mpa to 11.3 Mpa . The maximum petrophysical constraint in accumulation period under the formation temperature of 125℃ is $0.058\times10^{-3}\mu m^2$. All types of reservoirs can accumulate hydrocarbon.

With fault -the surplus pressure is the main accumulation dynamics. The surplus pressure is 1.8 Mpa to 12.6 Mpa . The maximum petrophysical constraint in accumulation period under the formation temperature of 125℃ is $0.037\times10^{-3}\mu m^2$. All types of reservoirs can accumulate hydrocarbon.

property and dynamics of a reservior in accumulation period

- The dynamics and physical property coupled with regard to hydrocarbon accumulation period

Petrophysical constraint

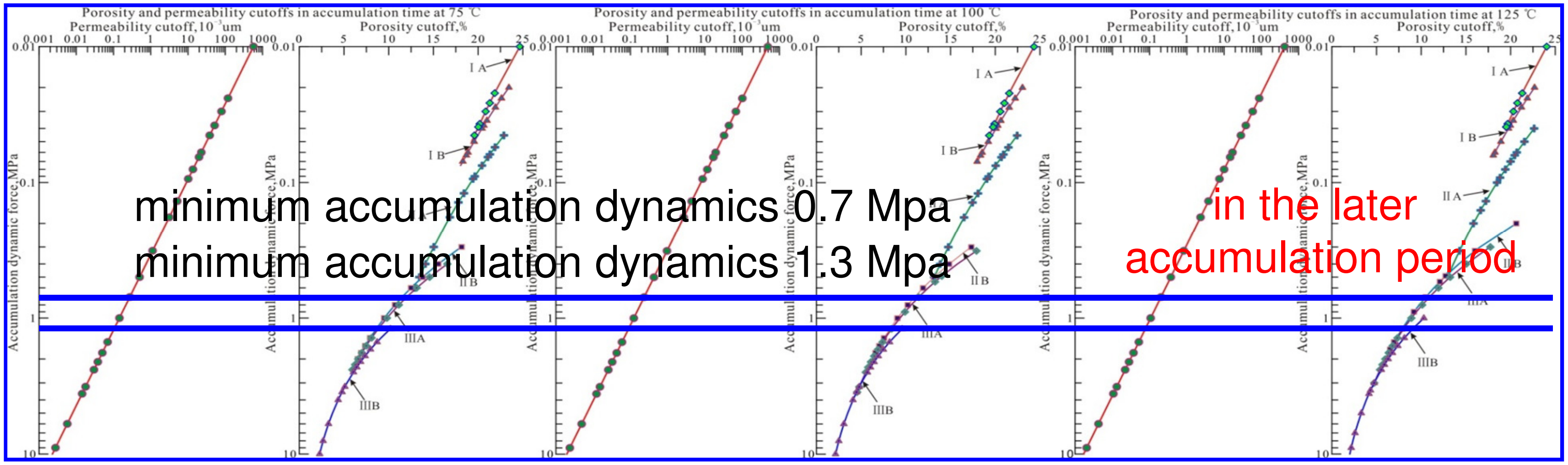

0.015×10^{-3}μm^2 to 62×10^{-3}μm^2 in the later accumulation period

no fault- the pressure generated by hydrocarbon generation is 0.7 Mpa to 12.7 Mpa . The petrophysical constraint is from 0.001 to 0.203×10^{-3}μm^2 . Reservoir with diagenetic facies (A) and diagenetic facies (B) don't develop accumulation conditions in low accumulation dynamic.

With fault -the surplus pressure is 1.3 Mpa to 16.2 Mpa . The petrophysical constraint is from 0.0007 to 0.066 ×10^{-3}μm^2. Reservoir with diagenetic facies (A) and diagenetic facies (B) don't develop accumulation conditions in low accumulation dynamic.

property and dynamics of a reservior in accumulation period

➢ Distribution of hydrocarbon resources

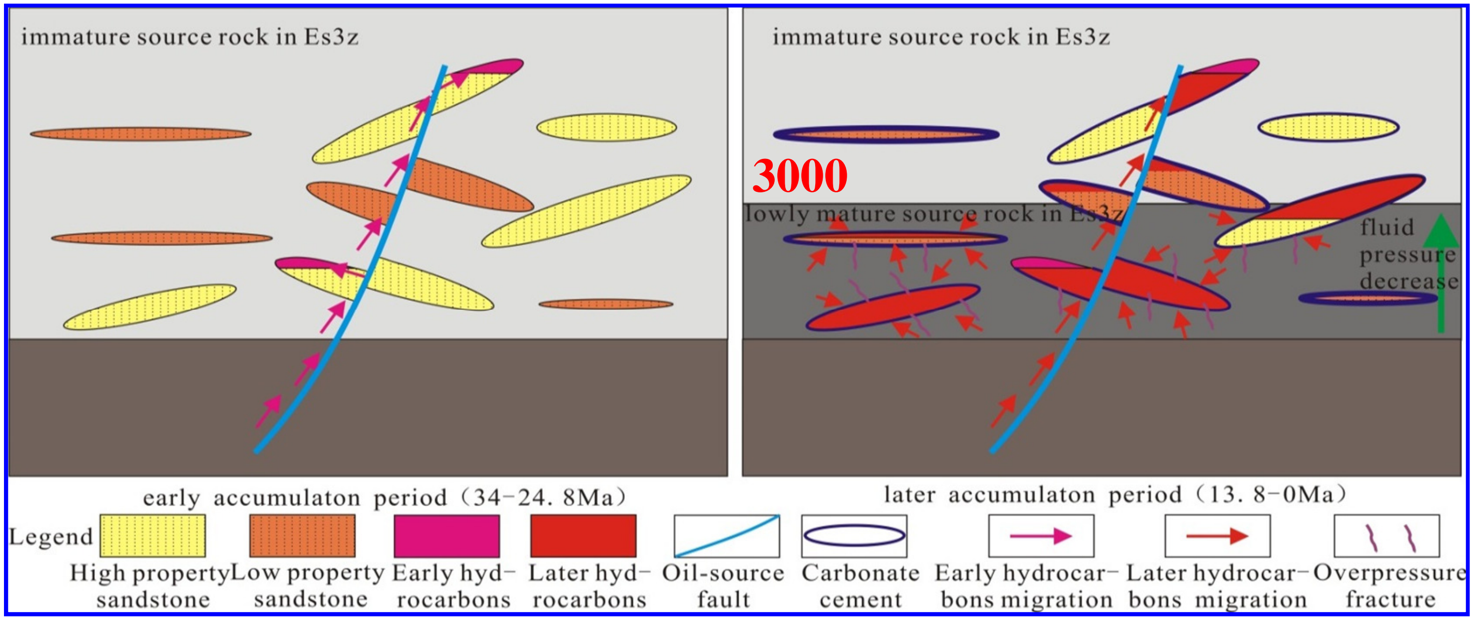

The hydrocarbon accumulation patterns of low permeability turbidite reservoirs

- **in the early accumulation period :the sand body with oil source fault development connected with source rock is easy to accumulate hydrocarbon.**

- **in the later accumulation period :**
  - **The hydrocarbon-filling degree is higher when the burial depth of turbidite reservoirs is more than 3000 m. The isolated lenticular sand bodies can accumulate hydrocarbon.**
  - **When the burial depth of turbidite reservoir is less than 3000 m, the isolated lenticular sand bodies cannot accumulate hydrocarbon.**

property and dynamics of a reservior in accumulation period

- Distribution of hydrocarbon resources

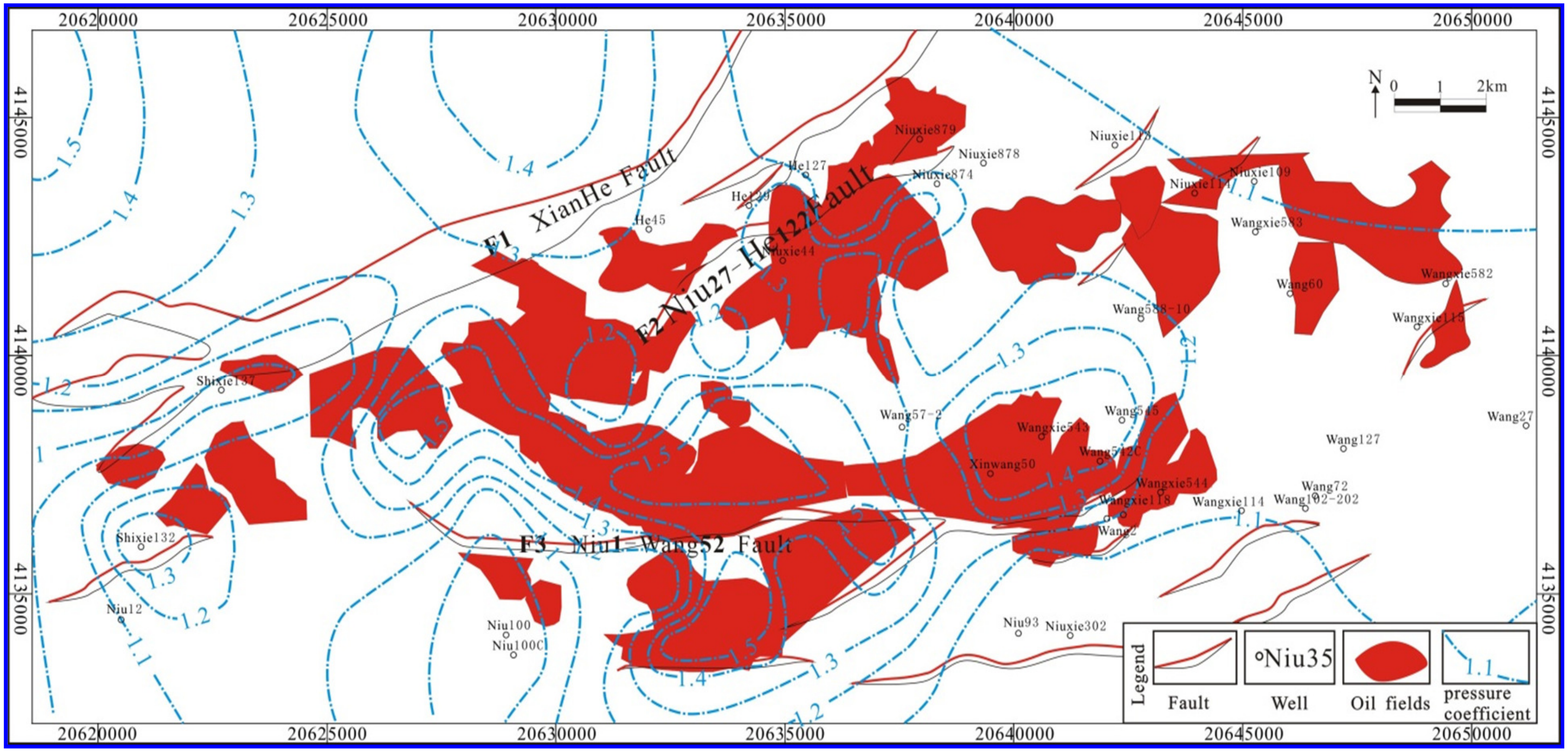

The hydrocarbon distribution regularities of the low permeability turbidite reservoirs of Es3z in Dongying sag

The oil-source faults controlled the accumulation of reservoirs. For flat surface, taking Niuzhuang subsag as example, hydrocarbon always accumulated in reservoirs around the oil-source faults and areas near the center of subsag with high accumulation dynamics.

Conclusions

- Turbidite sandstones from Es3z in Dongying Sag are mostly lithic arkoses, and composed of mainly fine to medium sized grains. Low permeability reservoirs with middle to high porosity are most common, the reservoir space is mainly primary. There are six types of pore throat structures. The major diagenetic events observed are mechanical compaction, cementation, metasomasis and dissolution.

- The paragenesis diagenetic minerals noted in this study are determined: Siderite/micritic carbonate→first dissolution of feldspar →the beginning of first hydrocarbon filling→first quartz overgrowth/authigenic kaolinite precipitation→the second period of carbonate cementation→the finish of first hydrocarbon filling→dissolution of quartz/feldspar overgrowth→second dissolution of feldspar and carbonate cementation→the beginning of second hydrocarbon filling→second quartz overgrowth/authigenic kaolinite precipitation→the third period of carbonate cementation/pyrite cementation. Compaction existed throughout the whole burial and it is an evolutional process.

Conclusions

- Except reservoirs with diagenetic facies(A), other turbidite reservoirs from Es3z in Dongying sag during the early accumulation period are middle to high permeability ranging from $10\times10^{-3}\mu m^2$ to $4207.3\times10^{-3}\mu m^2$, and all types of reservoirs can accumulate hydrocarbon. In the later accumulation period, except those with diagenetic facies(C) other reservoirs are all low permeability ones ranging from $0.015\times10^{-3}\mu m^2$ to $62\times10^{-3}\mu m^2$, and all types of reservoirs can form hydrocarbon accumulation with high accumulation dynamics. Reservoir with diagenetic facies (A) and diagenetic facies (B) don't develop accumulation conditions with low accumulation dynamics.

- The hydrocarbon-filling degree is higher when the burial depth of turbidite reservoirs is more than 3000 m. The isolated lenticular sand bodies can accumulate hydrocarbon. When the burial depth of turbidite reservoir is less than 3000 m, the isolated lenticular sand bodies cannot accumulate hydrocarbon. Hydrocarbons have been always accumulated in reservoirs around the oil-source faults and areas near the center of subsag with high accumulation dynamics.


Thank You !